

# A method to improve the reliability and the fatigue life of power device substrates

S. Pietranico<sup>1,2</sup>, S. Pommier<sup>1</sup>, S. Lefebvre<sup>2</sup>, S. Pattofatto<sup>1</sup>

<sup>1</sup> *LMT-Cachan*, <sup>2</sup> *SATIE*, (ENS Cachan/CNRS/UPMC/UniverSud Paris), 61, avenue du Président Wilson, 94235 Cachan, France

**Abstract:** Electronic power devices used for transportation applications (automotive and avionics) experience severe temperature variations which promote their thermal fatigue and failure. For example, for power modules mounted on the engine of an aircraft, temperature variations range from  $-55^{\circ}\text{C}$  (in the worst case of storage before takeoff) to  $+200^{\circ}\text{C}$  (flight). The studied modules are composed of direct bonded copper (DBC) substrates which allow isolating the active parts of the module (silicon dies) from their base plates. The failure occurs in DBC substrates, which are copper/ceramic/copper sandwiches. The Weibull approach was used to model the brittle fracture of the ceramic layer from a natural defect. Using the finite element method, it was possible to analyse how a thermal loading history may modify the risk of failure of the DBC substrate. It was shown, in particular, that three overcooling cycles should produce an “overload retardation effect”. Experimentally, applying 3 “overload cycles” ( $-70^{\circ}\text{C}, +180^{\circ}\text{C}$ ), before applying usual thermal fatigue cycles ( $-30^{\circ}\text{C}, +180^{\circ}\text{C}$ ), increased very significantly the fatigue life of a set power modules. This result shows that the fatigue life and the reliability of power electronic devices could be optimized using a thermo-mechanical approach of the problem and suitable failure criteria.

## 1. INTRODUCTION

Power semiconductor modules are mainly used for controlling electric motors, especially in transportation applications (automotive and avionics). Improving the reliability and the fatigue life of high power electronic devices is a real challenge for these applications in which power modules are increasingly used, in particular for purposes of reducing engines consumption. In many of these applications, power modules experience cyclic temperature variations. Two types of thermal cycles are superimposed, power cycles stemming from electric current in the active parts of the modules during the phases of operation and hence in temperature variations (Joule effect) and passive cycles stemming from ambient temperature variations. In the environment of an aircraft engine, these variations are typically between  $-30^{\circ}\text{C}$  and  $+180^{\circ}\text{C}$  and in the worst case between  $-55^{\circ}\text{C}$  to  $200^{\circ}\text{C}$ . Therefore, power electronic devices are highly vulnerable to variable amplitude thermal fatigue. The aim of this research is to understand the mechanisms at the origin of failure and to model them so as to optimize either the geometry or the manufacturing process in order to improve their fatigue life and their reliability

The studied modules are composed of chips, ceramic substrates and base plate. Chips are soldered on ceramic substrates which are themselves soldered on base

plates. Ceramic substrate ensures the electrical insulation of the chips from the base plate. The substrate must also allow the evacuation of the heat resulting from power dissipation, from chips to the base plate. For this purpose, Direct Bonded Copper (DBC) substrates are commonly used in power modules, because of their good thermal conductivity. They are composed of a ceramic layer (AlN or Si<sub>3</sub>N<sub>4</sub>) with a thin sheet of copper bonded to both sides by a high-temperature oxidation process. The top copper layer (thickness  $t_{Cu1}=127 \mu\text{m}$  to  $300\mu\text{m}$ ) is chemically etched on the upper layer so as to form an electrical circuit, the ceramic tile (thickness  $t_{cer}=635 \mu\text{m}$ ) ensures the electrical insulation, while the bottom copper layer is kept plain and soldered to the base plate (copper or AlSiC) mounted on a heat spreader. The global thermal expansion coefficient of a DBC substrate is close to that of a silicon chip which reduces the effect of thermal cycling at the interface between the chip and the substrate. Conversely, and especially for the highest temperature variations, thermal fatigue failures appear inside the DBC substrate and limit the fatigue life of the module. It was observed that cracks are either initiated from the layer of ceramics or from geometric singularities in the DBC substrate [1,10]. In the latter case, tiny fatigue cracks grow cycle by cycle at the interface between the upper copper layer and the ceramic layer. When a crack has reached a critical size, it bifurcates and breaks the ceramic layer [10]. The two mechanisms compete to break the DBC substrate and are examined independently. This paper is devoted to the first failure mechanism, i.e. a brittle fracture from the ceramic layer. This failure mechanism was characterized experimentally and a finite element model of a DBC substrate was set so as to propose a method to improve the fatigue life of the modules. This solution was tested experimentally.

## 2. MATERIAL'S PROPERTIES.

First of all, we characterized the materials composing the DBC substrates. Two types of ceramics were tested (AlN or Si<sub>3</sub>N<sub>4</sub>). The behaviour of the copper sheet was also characterized.

### 2.1 Ceramic's Properties

The brittle fracture of the ceramic layer can occur from a material defect of the ceramic itself such as a grain boundary, a micro-crack or a pore. These defects being statistically distributed in the ceramic layer, their fracture strength is also statistically distributed. A probabilistic approach is therefore employed as a fracture criterion from natural defects in the ceramic layer.

#### 2.1.1 WEIBULL LAW

To represent the random nature of the tensile strength to failure of the material, the Weibull law and the weakest link theory are employed:

$$P_F = 1 - P_S = 1 - \exp\left(-\frac{dV}{V_o}\left(\frac{\sigma}{\sigma_0}\right)^m\right) \quad (1)$$

The probability of failure  $P_F$  is function of the maximum positive principal stress  $\sigma$  in a given volume of material  $dV$ .  $V_o$  is used to non-dimension the volume

$dV$  of tested material and is fixed arbitrarily at  $V_o = 1\text{mm}^3$ . Experiments were performed in order to identify  $\sigma_o$  and  $m$  for the AlN and the  $\text{Si}_3\text{N}_4$  ceramic used in the power modules.

### 2.1.2 EXPERIMENTS

Samples of ceramic of different geometries have been characterized. Three points bending tests were used for this purpose (Fig. 1). The distance  $L$  is equal to 19 mm in all cases. The thickness  $t$  of the AlN samples is either equal to 0.5 mm or 1 mm and their width  $w$  is either 2.5 mm or 5 mm. The thickness  $t$  of the  $\text{Si}_3\text{N}_4$  samples is equal to 0.3 mm and their width  $w$  is either 2.5 mm or 5 mm. In a three point bend test, the stress is calculated as follows as a function of the maximum stress  $\sigma_{\max}$  in ( $x = 0, y = t/2$ ):

$$\sigma(x, y) = \left(1 - \frac{2|x|}{L}\right) \frac{2y}{t} \sigma_{\max} \quad (2)$$

According to the weakest link theory, the survival probability of the sample is the product of the survival probability of each sub-volume inside the sample. Thus, taking into account the Weibull law (Eq. 1) the failure probability is as follows:

$$P_F(V) = 1 - P_S(V) = 1 - \exp \int_V -\frac{dV}{V_o} \left(\frac{\sigma(x, y)}{\sigma_o}\right)^m = 1 - \exp \left(-\left(\frac{\sigma_W}{\sigma_o}\right)^m\right) \quad (3)$$

Where:

$$\sigma_W = \sigma_{\max} \left(\frac{V_{\text{eff}}}{V_o}\right)^{1/m} \quad \text{and} \quad V_{\text{eff}} = \int_V \left(\frac{\sigma(x, y)}{\sigma_{\max}}\right)^m dV = \left(\frac{V}{2}\right) \frac{1}{(1+m)^2} \quad (4)$$

It is useful to use test samples with different geometries in order to determine precisely the effect of a volume change on the fracture strength. More than hundred specimens were broken to characterize the Weibull law. The broken samples are sorted by increasing values of  $\sigma_W$ , so as to determine their failure probability. Since  $\sigma_W$  is function of  $m$ ,  $m$  was optimized step by step so as to get finally all the results lying on the same curve.

Finally, a very good agreement is found between the set of experimental results and a Weibull law with  $m = 9.56$  and  $\sigma_o = 360\text{MPa}$  for Aluminium nitride.

Respectively, Weibull's parameters of the  $\text{Si}_3\text{N}_4$  are  $m = 13.72$  and  $\sigma_o = 470\text{MPa}$ . For the same probability of failure the tensile stress in  $\text{Si}_3\text{N}_4$  samples is higher than the stress in AlN samples but typically a hundred MPa.

It is important to mention that the smallest AlN (resp  $\text{Si}_3\text{N}_4$ ) effective volume used in these experiments is equal to  $0.07\text{mm}^3$  (resp  $0.03\text{mm}^2$ ). It is therefore possible to use this model to predict the failure probability of AlN (resp  $\text{Si}_3\text{N}_4$ ) for any volume of material larger than  $0.07\text{mm}^3$  (resp  $0.03\text{mm}^2$ ), but it is not safe to extrapolate this model to smaller volumes. Correspondingly, in the experiments, the maximum value of the stress gradient non-dimensioned by the maximum stress is equal to  $4\text{mm}^{-1}$ . When this law is used, the areas for which the stress

gradient is higher than  $4 \text{ mm}^{-1}$  should therefore be excluded of the analysis. This is the case in particular of the vicinity of the geometric singularities of the model.

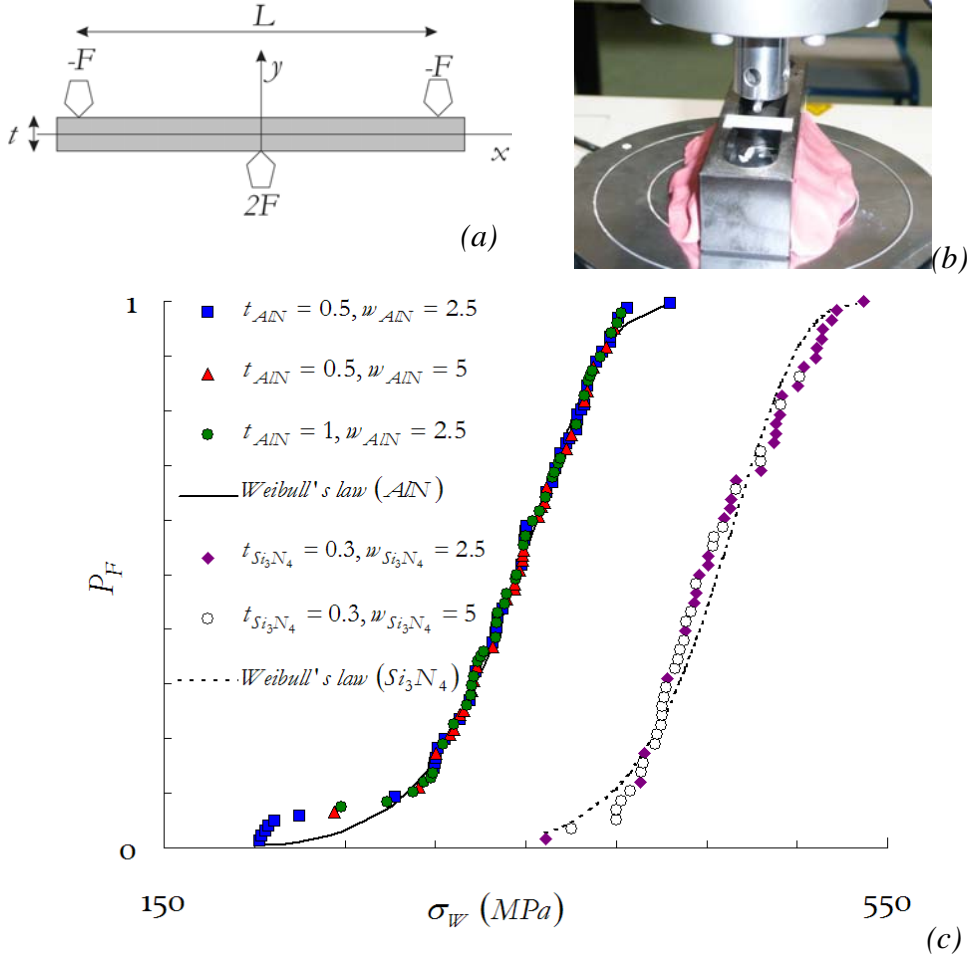


Figure 1: Three points bending test. (a) geometry. (b) experimental setup. (c) experimental results. The failure probability determined during the experiments is plotted versus the Weibull stress at failure.

## 2.2 Copper's Properties

The expansion coefficients and the Young's moduli were found in the literature. The expansion coefficient of copper varies between  $15.6 \cdot 10^{-6} / ^\circ\text{C}$  and  $18 \cdot 10^{-6} / ^\circ\text{C}$  between  $-50^\circ\text{C}$  and  $180^\circ\text{C}$ . This variation was neglected. The copper was assumed to be elastic-plastic with a non-linear Armstrong-Frederick kinematics and isotropic hardening law (Table 1). The Chaboche's model was used for this purpose [9], this material model is available in Abaqus standard.

The parameters  $E$ ,  $\nu$ ,  $R_0$ ,  $C$ ,  $\gamma$ ,  $Q$  and  $b$  of the copper constitutive model were determined using a tensile test and a cyclic tensile test performed on samples extracted from a thin sheet of copper ( $t = 127 \mu\text{m}$ ) used in DBC substrates (Fig. 2). Unfortunately, the geometry of the samples did not allow performing strain-imposed push-pull test. The identification of the coefficients  $C$ ,  $\gamma$ ,  $Q$  and  $b$ , that allow defining the kinematic and isotropic hardening laws of the material, is

therefore questionable, in particular Q and b, but at least simulations and experiments are in reasonable agreements. All these coefficients were assumed to remain constant between  $-50^{\circ}\text{C}$  and  $+180^{\circ}\text{C}$ , which is valid for the ceramics, but might be questionable for copper. More experiments are planned in the future to better characterize the cyclic behaviour of copper.

*Table 1: Material parameters employed for copper and AlN [2].*

|        |                               |          |                                 |
|--------|-------------------------------|----------|---------------------------------|
| Copper | Young's modulus               |          | 130 GPa                         |
|        | Poisson's ratio               |          | 0.24                            |
|        | Thermal expansion             |          | $16. 10^{-6} /^{\circ}\text{C}$ |
|        | Initial yield stress          | $R_0$    | 180 MPa                         |
|        | Kinematic hardening parameter | C        | 602600 MPa                      |
|        | Kinematic hardening rate      | $\gamma$ | 2300                            |
|        | Isotropic hardening amplitude | Q        | 30 MPa                          |
|        | Isotropic hardening rate      | b        | 100                             |
| AlN    | Young's modulus               |          | 320 GPa                         |
|        | Poisson's ratio               |          | 0.24                            |
|        | Thermal expansion             |          | $5. 10^{-6} /^{\circ}\text{C}$  |

It is worth to mention that, until now, finite element simulations are employed to give prominence to the main trends. It is not aimed at predicting the fatigue life of the component, for instance, but at indicating how the geometry or the manufacturing process should be modified so as to increase the resistance of the modules.

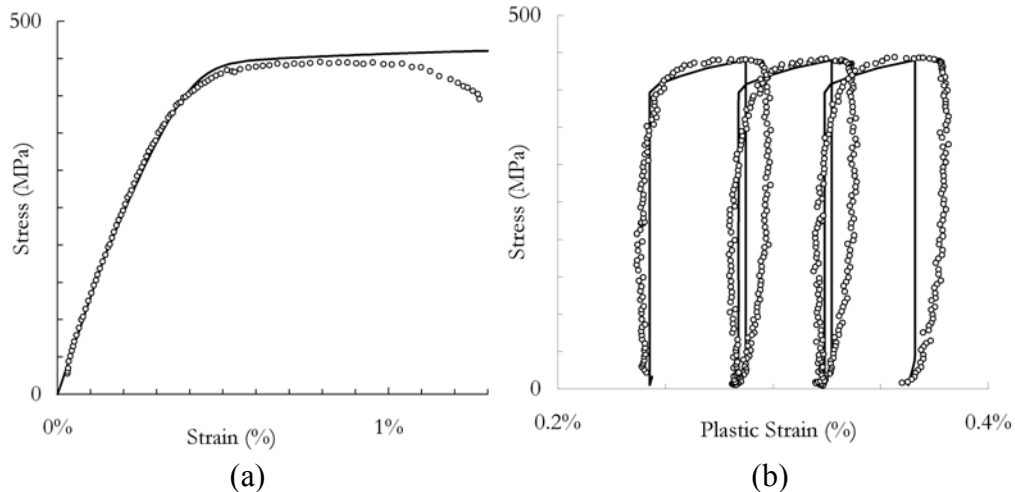


*Figure 2: Tensile tests. Thin sheet of copper employed in DBC substrates. The thickness of the sheet is  $127 \mu\text{m}$ . The strain is measured using a strain gauge. Symbols : Experiments, lines : Simulations. (a) strain controlled monotonic tensile test and (b) stress controlled cyclic tensile test, the minimum stress is 10 MPa, the maximum stress is increased by 10 MPa every three cycles.*

### 3. FINITE ELEMENT MODEL.

We used the finite element method and the code Abaqus.

For this purpose, the thickness of the layer of ceramic was set equal to 635  $\mu\text{m}$ , the thickness of the upper layer of copper was fixed at 300  $\mu\text{m}$ , while the other is fixed at 400  $\mu\text{m}$ . The mesh size varies from 30 $\mu\text{m}$  down to 1 $\mu\text{m}$  at the geometric singularities (Fig. 3). 2D axisymmetric conditions are employed.

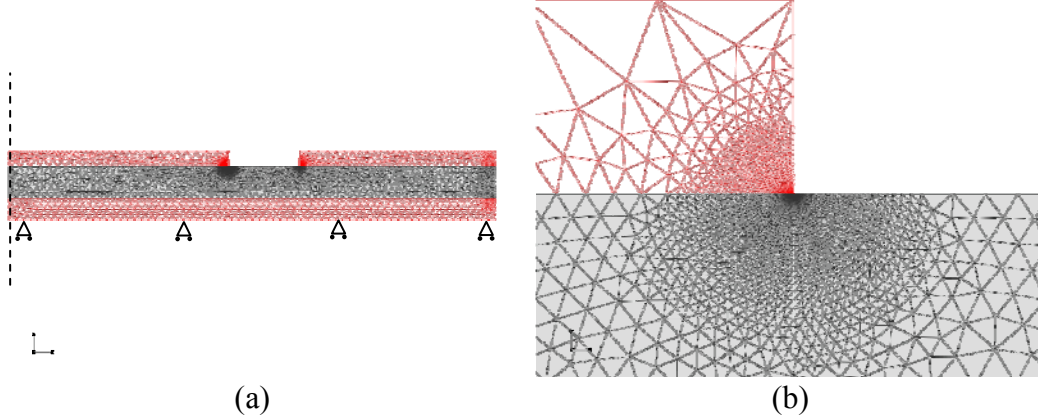


Figure 3: (a) FE model of the DBC substrate and boundary conditions (b) detail of the mesh around a geometric singularity

#### Hypotheses

Real DBC substrates display notches, created by chemical etching of the upper layer of copper, that modify significantly the stress field inside the ceramic layer. Therefore, a finite element model is set up, that uses a more realistic geometry for the DBC substrate and a suitable elastic-plastic constitutive model for copper. The Weibull criterion is then used to post-treat finite element computations. The Weibull law is applied to each element of the ceramic layer and the weakest link theory is employed to cumulate the failure probabilities:

$$P_F(V) = 1 - P_S(V) = 1 - \exp\left(-\sum_{i=1}^N \frac{V_i^{EF}}{V_o} \left(\frac{\langle \sigma_i^{EF} \rangle}{\sigma_0}\right)^m\right) \quad (8)$$

Where  $V_i^{EF}$  is the volume of the  $i^{th}$  element and  $\langle \sigma_i^{EF} \rangle$  is the positive part of the maximum principal stress in that element. In these computations, the mesh size is adjusted so that the volume of each element remains higher than 0.07  $\text{mm}^3$  in the major part of the model.

Besides, the notches created by chemical etching are sharp and can be considered as geometric singularities. Actually, stresses and strains at the notch roots do not converge when the mesh size diminishes. In these areas the mesh size is highly refined (Fig. 3 b) so as to analyze the problem using a LEFM based approach [8]. Using FE computations, it is found that the maximum principal stress gradient is higher than  $4 \text{mm}^{-1}$  if the distance of the element to a geometric singularity is typically below 100  $\mu\text{m}$ . Since the Weibull law was characterized experimentally only for stress gradients below this value, the elements at a distance below 100

$\mu\text{m}$  from a geometric singularity (Fig. 3 a) are excluded when the failure probability is calculated (Eq. 8). In return, the elements excluded for the calculation of the failure probability by the Weibull approach are used in a LEFM based failure criteria [10].

This restriction makes sense since the Weibull approach is used to determine the risk of failure from natural defects of the ceramic and applies only in areas where stress and strain gradients remain moderate. When the stress gradient is large, in the vicinity of a geometric singularity, that singularity is assumed to be a much more efficient initiation site than a natural defect. In such a case, a LEFM based criterion [8] should be used in preference to a Weibull law.

### Results

The computations were performed for the two ceramics ( $\text{AlN}$ ,  $\text{Si}_3\text{N}_4$ ). The effect of thermal overload on subsequent cycles was studied numerically. The DBC substrates were submitted to three cycles at  $T_{\min}=-70^\circ\text{C}$  and  $T_{\max}=180^\circ\text{C}$  before applying thermal fatigue cycles with  $T_{\min}=-30^\circ\text{C}$  and  $T_{\max}=180^\circ\text{C}$ . The “overloads” increase the probability of failure of the ceramic during overload cycles, but then, during thermal fatigue cycles, the probability of failure is significantly lower if the DBC substrate has experienced overloads by comparison with DBC substrates that have experienced thermal fatigue cycles only. The probability of failure is divided by typically a factor two.

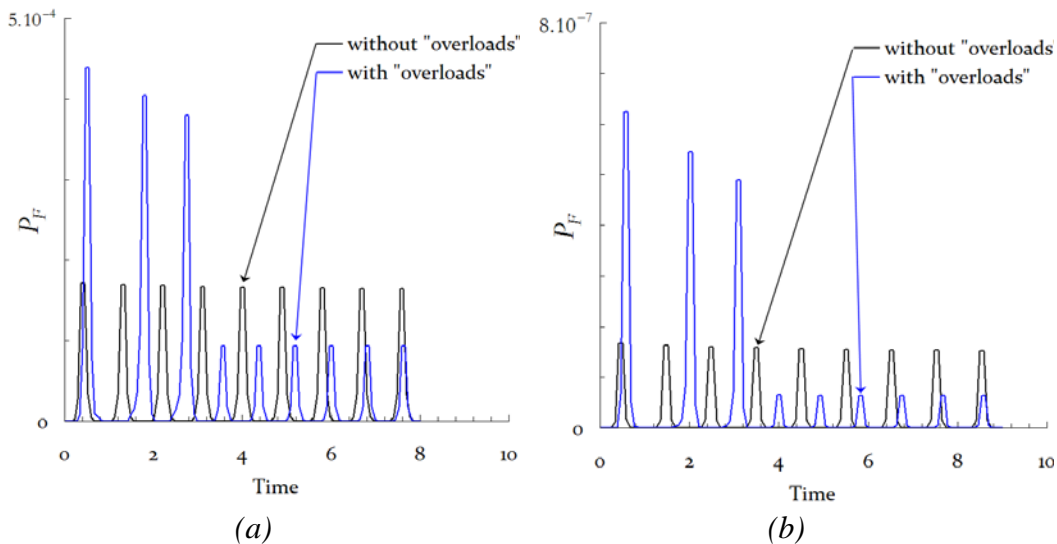


Figure 4: Probability of failure with or without “overloads” (a)  $\text{AlN}$  (b)  $\text{Si}_3\text{N}_4$

### 4. EXPERIMENTS.

Even if numerical results remain qualitative only because the cyclic elastic-plastic behaviour of the copper sheet is not precisely known, they indicate that applying a few “overloads” cycles before cycling should improve the resistance to failure of DBC substrates.

Therefore, experiments were also conducted to evaluate the effect of such overload cycles on the fatigue life of DBC substrates. The DBC substrates were

submitted to three cycles at  $T_{\min}=-70^{\circ}\text{C}$  and  $T_{\max}=180^{\circ}\text{C}$  before applying usual thermal cycles with  $T_{\min}=-30^{\circ}\text{C}$  and  $T_{\max}=180^{\circ}\text{C}$ . A set of 17 substrates were tested simultaneously. The capacitance was measured periodically (Fig. 5). This experiment can be directly compared with that performed by Dupont [1] using the same substrates and the same thermal cycles except those including overloads.

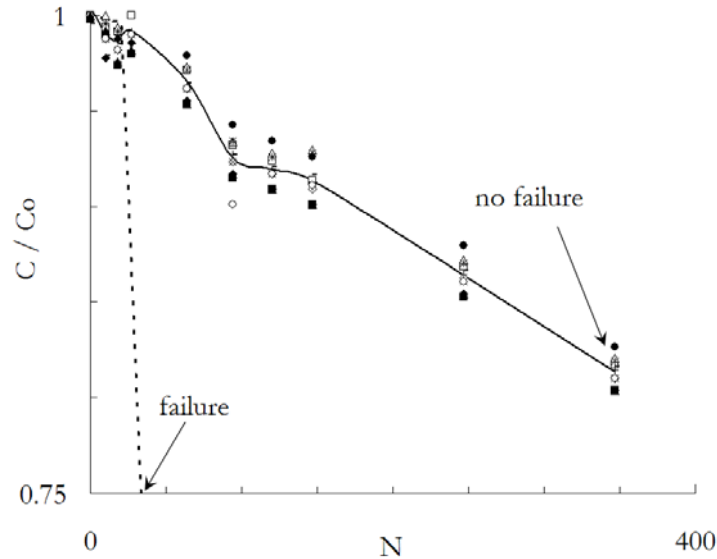


*Figure 5: Evolution of the capacitance  $C$  (pF) versus the number of thermal fatigue cycles, non-dimensional by the initial capacitance  $C_0$ . Thick line and symbols, three initial “overloads cycles” are applied ( $T_{\min}=-70^{\circ}\text{C}$  and  $T_{\max}=180^{\circ}\text{C}$ ) before usual thermal fatigue cycling ( $T_{\min}=-30^{\circ}\text{C}$  and  $T_{\max}=180^{\circ}\text{C}$ ). After 347 cycles the samples have not failed. Dotted lines: without overloads [1] : the failure occurs between the 40<sup>th</sup> and the 50<sup>th</sup> cycle.*

The results are plotted in Fig. 5. A considerable increase of the fatigue life is obtained. While the fatigue life was ranging between 40 and 50 cycles for usual thermal fatigue cycles, it grows over 350 cycles if three overloads thermal cycles are applied before applying usual thermal fatigue cycles.

The second interesting result is that the capacitance diminishes progressively which indicates the growth of a crack at the interface. This may allow monitoring the fatigue crack growth rate in service.

In practice, other technologies can be used to increase the fatigue life of the substrates (dimples...) but these results indicate that very simple methods that take advantage of the thermo-mechanical properties of the materials are also very efficient.

## 5. DISCUSSIONS

The second mechanism of failure considered here is the brittle fracture of the ceramic layer initiated from a small fatigue crack close to the upper interface between copper and ceramic. At the singularities created by chemical etching, stresses and strains are extremely high. Therefore, a crack initiation or a failure criterion based on local stresses or strains in the element cannot be applied to this

problem. As a matter of fact, in linear elastic media, not only crack tips but also vertices of internal corners are singular [4,5]. Similar configurations are also encountered in contact problems [6, 7]. In those cases, it was shown that the stress field can be represented by the product of a shape function  $r^\lambda f(\theta)$  and of a generalized stress intensity factor [8]. Various authors [6,7] have employed generalized stress intensity factors successfully to characterize stress fields in the vicinity of singularities that are not cracks.

In 1971, Bogy [5] derived an analytical solution for an internal corner which vertex located at an interface between two semi-infinite elastic materials. This solution allows determining the order of the singularity  $\lambda$  of the stress field in the vicinity of the vertex. This problem is the subject of another publication [10]. To briefly summarize, we showed that in this case  $\lambda$  is close to  $1/2$ , which allows extracting the intensity factors for this problem using the Westergaard's functions. This method was used to post-treat finite element computations and it was shown that the application of overloads reduces significantly the "stress intensity factors" at the geometric singularities.

#### **CONCLUSIONS AND PROSPECTS**

The thermo-mechanical behaviour of DBC substrates for electronic devices was studied using the FE method. These substrates are submitted to thermal fatigue. The final objective is to propose a method to optimize the geometry and the materials in the DBC substrate so as to maximize its fatigue life and its reliability. First of all the failure probability of the ceramic layer was modelled by a Weibull law. To identify the parameters  $m$  and  $\sigma_0$  of the AlN layer (resp Si<sub>3</sub>N<sub>4</sub>), three points bending tests were performed for three samples geometry in order to identify precisely the volume change effect on the failure probability of each material. A good agreement is found between the Weibull law and the set of experimental results, with  $m=9.56$  (resp  $m=13.72$ ) and  $\sigma_0=360$  MPa (resp  $\sigma_0=470$  MPa),  $V_0$  being set at  $1 \text{ mm}^3$ . This law can be used as a post-treatment routine of FE computation so as to determine the risk of failure of the AlN layer from a natural defect of the ceramic.

Finite element computations were performed to analyze the effect of "thermal overload" cycles on the probability of failure of the ceramic layer. Besides, experiments have shown that the application of three thermal overloads before applying thermal fatigue cycles was at the origin of a very significant increase of the fatigue life of the DBC substrate. These results are consistent with the trends indicated by the simulations that need to be enriched so as to account for crack initiation and growth at geometric singularities..

#### **Acknowledgements**

The author would like to acknowledge the French Research Agencies (DGA and CNRS) and the Farman institute of the Ecole Normale Supérieure de Cachan for their financial support and their encouragements to set up interdisciplinary research programs.

## References

- [1] L. Dupont, Thèse de Doctorat de l'ENSC, « Contribution à l'étude de la durée de vie des assemblages de puissance ... », juin 2006.
- [2] Y. Nagatomo and T. Nagase, "The Study of the Power Modules with High Reliability for EV Use", 17th EVS conf., Montreal, October 2000.
- [3] A. Houssam, et al, "Room temperature tensile and flexural strength of ceramics in AlN-SiC system" J. of the Eur. Cer. Soc., Vol. 15, I. 5, 1995, pp 425-434.
- [4] Khrapkov AA. The first basic problem for a notch at the apex at an infinite wedge. Int J Fract 1970,7(4):373-82.
- [5] Bogy D.B. On the plane elastostatic problem of a loaded crack terminating at a material interface, J.Appl.Mech., 38, 1971, 911-918.
- [6] Giannakopoulos A.E, Lindley T.C, Suresh S. Aspects of equivalence between contact mechanics: Theoretical connections and a life-prediction methodology for fretting-fatigue, Overview, 129, 1997, 2955-2968.
- [7] Johnson K.L, Contact Mechanics, Cambridge University Press, Cambridge, 1985.
- [8] D. Leguillon, Strength or toughness? A criterion for crack onset at a notch , EJMA-S E, Volume 21, Issue 1, 2002, Pages 61-72.
- [9] J. Lemaître, J.-L. Chaboche, Mécanique des matériaux solides, Dunod, Paris (1985)
- [10] S. Pietranico, S. Lefebvre, S. Pommier, Z. Khatir, Conf: EPF 2008 , XIIème colloque Electronique de Puissance du Futur, 2 et 3 juillet 2008, Tours, France